0021-972X/03/$15.00/0
Printed in U.S.A.

The Journal of Clinical Endocrinology & Metabolism 88(8):3902–3912

doi: 10.1210/jc.2003-030174

Identification of Steroid Sulfate Transport Processes in the Human Mammary Gland

F. PIZZAGALLI, Z. VARGA, R. D. HUBER, G. FOLKERS, P. J. MEIER, AND M. V. ST-PIERRE

Division of Clinical Pharmacology and Toxicology (F.P., R.D.H., P.J.M., M.V.S.-P.), Department of Internal Medicine, and Department of Pathology (Z.V.), University Hospital of Zürich; and Institute of Pharmaceutical Chemistry (F.P., R.D.H., G.F.), Department of Applied Biosciences, Swiss Federal Institute of Technology, Zürich 8091, Switzerland

Circulating hormones and local biotransformation of steroid precursors are both sources of estrogen in human mammary tissue. Estrone-3-sulfate (E_1S) is an important estrogenic form in premenopausal women, and dehydroepiandrosterone sulfate (DHEAS) constitutes a major adrenal precursor. Membrane transport systems that govern delivery of these anionic steroid conjugates to the mammary gland were investigated. RNA was screened by RT-PCR and Northern blotting for expression of organic anion transporting polypeptide (OATP) (solute carrier family 21A) and organic anion transporter (OAT) (solute carrier family 22A) gene families. OATP-B (*SLC21A9*) was the major carrier expressed; OATP-D (*SLC21A11*) and OATP-E (*SLC21A12*) were less abundant. In normal sections, OATP-B immunolocalized to the myoepithelium that surrounds the ductal epithelial cells. In invasive carcinoma, ductal epithelial cells were positive. OATP-B was characterized in stable transfected Chinese hamster ovary cells. E_1S affinity constant (K_m) [K_m = 5 μmol/liter, maximum velocity (V_{max}) V_{max} = 777 pmol/mg·min] and DHEAS (K_m = 9 μmol/liter, V_{max} = 85 pmol/mg·min) were substrates. The prostaglandins (PG) A_1 and PGA_2 stimulated uptake of E_1S and DHEAS by increasing V_{max} 2-fold but not changing K_m. The effect of PGA was selectively blocked by the lipophilic thiol reagent N-ethylmaleimide but not by the hydrophilic acetamido-4′(iodoacetyl)aminostilbene-2,2′-disulfonic acid, suggesting an interaction between the electrophilic cyclopentenone ring and specific cysteine residues of OATP-B. (*J Clin Endocrinol Metab* 88: 3902–3912, 2003)

THE MAMMARY GLAND is an estrogen-responsive tissue. Estrogens act through the estrogen receptors to direct normal lobular development, regulate epithelial cell growth, and increase the expression of steroid hormone metabolizing enzymes (1, 2). Moreover, estrogen is the most important etiological factor that supports the growth of estrogen receptor-positive breast tumors. One source of estrogen is local biosynthesis within the epithelial cells and stromal fibroblasts from the adrenally derived precursors, dehydroepiandrostenedione (DHEA) and androstenedione. DHEA circulates primarily in its 3β-sulfate form, dehydroepiandrosterone sulfate (DHEAS), and serves as the principal conjugated prohormone for the biosynthesis of both estrogenic [17β-estradiol (E_2), estrone (E_1), and 5-androstenediol] and androgenic (testosterone) steroids in peripheral tissues (3, 4). The enzymes that catalyze the desulfation of DHEAS, the subsequent 3β oxidation of DHEA to androstenedione and 17β reduction of androstenedione to testosterone, as well as the aromatization of testosterone and androstenedione into E_2 and E_1, respectively, have all been detected in breast tissue and studied in breast cancer cell lines (5–7). A second source of estrogen are the circulating hormones, the composition and concentration of which vary widely as a function of age. In premenopausal women, estrone 3-sulfate (E_1S) is the major form, and its cyclical concentrations range from 2.5 to 15 nmol/liter (8, 9). In breast tissue, E_1S is sequentially desulfated and reduced to the more potent E_2 (7, 10). In postmenopausal women, the estrogen concentrations decline, although adrenally derived DHEAS levels can remain above 2–3 μmol/liter even into the seventh decade (11).

The activities of several key enzymes necessary for *in situ* estrogen production are higher in tumors compared with normal tissue (12, 13), in keeping with the widely held tenet that sex steroid exposure is a strong risk factor for breast cancer. There are also epidemiological data to support an association between the circulating concentrations of hormones and prohormones, including E_1S and DHEAS, and the eventual risk of developing breast cancer, especially in the postmenopausal years (14, 15). This link implies that steroids in their sulfated, anionic form gain access to the intracellular milieu and can determine the extent of exposure to downstream, biologically active hormones. Sulfated steroid conjugates carry a net negative charge at physiological pH levels, and as such, their transfer across cell membranes is carrier mediated. Steroid sulfates have been identified as substrates for distinct members of two organic anion carrier gene families: the organic anion transporting polypeptide (OATP) superfamily, classified within the solute carrier 21A gene family (*SLC21A*) (16) and the organic anion transporter (OAT) family, encoded by the solute carrier 22A (*SLC22A*) genes (17). OATPs are multispecific transporters expressed in many tissues, including the liver, brain, and placenta, where they mediate the Na^+-independent uptake of a host of organic anionic compounds. In particular, OATP-A (*SLC21A3*) (18), OATP-B (*SLC21A9*) (19), the liver-specific

Abbreviations: CHO, Chinese hamster ovary; DAPI, 4′-6-diamidino-2-phenylindole; DHEA, dehydroepiandrostenedione; DHEAS, dehydroepiandrosterone sulfate; E_1, estrone; E_1S, estrone 3-sulfate; E_2, 17β-estradiol; IASD, acetamido-4′-(iodoacetyl)amino-stilbene-2,2′-disulfonic acid; K_m, affinity constant; NEM, N-ethylmaleimide; OAT, organic anion transporter; OATP, organic anion transporting polypeptide; PG, prostaglandin(s); SSC, saline sodium citrate; V_{max}, maximum velocity.

OATP-C (*SLC21A6*) and OATP-8 (*SLC21A8*) (20, 21), OATP-E (*SLC21A12*) (22), and OATP-F (*SLC21A14*) (23) have all shown convincingly that they accept selected conjugated steroids as substrates. Four isoforms of the OAT carrier family have been characterized. Of these, OAT3 (*SLC22A8*) and OAT4 (*SLC22A11*) mediate the cellular uptake of certain steroid conjugates in the kidney, liver, brain, and placenta (24–26).

Because the transport processes operative in mammary tissue will govern the cellular entry of conjugated steroids, it follows that individual carrier proteins may, in part, be determinants of downstream estrogen exposure in target cells. Accordingly, the identification and characterization of the relevant transporters present in human mammary epithelia deserve a detailed investigation. The aim of this study was to identify and characterize the organic anion uptake systems for conjugated steroids. Our findings show that OATP-B (*SLC21A9*) may be the most functionally relevant steroid sulfate carrier present and is able to account for delivery of both E_1S and DHEAS to normal and tumor breast tissue.

Materials and Methods

Materials

[6,7-^{3}H]-E_1S (53 Ci/mmol), [^{3}H]-DHEAS (60 Ci/mmol), and [^{3}H]-pregnenolone sulfate (389 mCi/mmol) were purchased from NEN Life Science Products (Boston, MA). [5,6-^{3}H]-PGE_1 (48 Ci/mmol) was purchased from Amersham Biosciences (Freiburg, Germany). [^{3}H]-PGA_1 was prepared by acid-catalyzed dehydration of [5,6-^{3}H]-PGE_1 and purified by thin-layer chromatography, as described by Andersen (27). All cell culture media and reagents were obtained from Life Technologies (Paisley, UK) or Sigma-Aldrich Chemie (Steinheim, Germany). Steroids used in inhibition studies were obtained from Steraloids (Newport, RI); prostaglandin (PG) A_1 and A_2 were purchased from Alexis Corporation (Lausen, Switzerland); and unlabeled PGE, 2-cyclopenten-1-one, and N-ethylmaleimide (NEM) were purchased from Sigma-Aldrich Chemie (Steinheim, Germany). Acetamido-4′-(iodoacetyl)amino-stilbene-2,2′-disulfonic (IASD) acid was purchased from Molecular Probes (Eugene, OR). All other chemicals and reagents were of analytical grade and are available from commercial sources.

RT-PCR

Expression of the known members of the OATP and OAT gene superfamilies in normal human mammary tissue was studied by RT-PCR assay. Reverse transcription was performed using total RNA (Clontech, Palo Alto, CA) primed with Oligo$(dT)_{15}$ as a template and AMV Reverse Transcriptase (Promega, Wallisellen, Switzerland). PCR amplification used primers specific for each transporter (Table 1) and the following conditions: one cycle of 95 C for 2 min; 40 cycles of 95 C for 45 sec; primer-specific annealing temperature for 45 sec; 72 C for 1 min; and a final elongation of 72 C for 5 min. The primer-specific annealing temperature was 50 C for OATP-A, OATP-C, OATP-D, OATP-E, OATP-F, and OATP8, 58 C for hPGT, 63 C for OATP-B, and 55 C for all OATs.

Northern blot analysis

Twenty micrograms of normal human mammary gland total RNA (Clontech) per lane were loaded on a 1% agarose-formaldehyde gel. After electrophoresis, the gel was washed three times for 10 min in 10× saline sodium citrate (SSC) and transferred overnight in 20× SSC to a Hybond-NX (Amersham Biosciences) nylon membrane. The blot was prehybridized for 30 min at 68 C in ULTRAhyb (Ambion, Austin, TX) and hybridized overnight at 68 C in the same buffer with a ^{32}P-labeled antisense-RNA probe (nucleotides of the published sequences: OATP-A nts 1959–2614, accession no. NM_134431; OATP-B nts 266–984, accession no. NM_007256; OATP-D nts 1742–1905, accession no. NM_013272; OATP-E nts 1251–1551, accession no. NM_016354; OATP-F nts 1–545, accession no. AF260704, with a specific activity of 1.4 counts per minute × 10^6/ml. The blots were washed twice for 5 min with 2× SSC/0.1% SDS at 68 C, twice for 15 min with 0.1× SSC/0.1% SDS at 68 C, and then exposed to autoradiography film at −70 C with an intensifying screen, for 2 d for OATP-B and 5 d for OATP-A, OATP-D, OATP-E, and OATP-F.

Immunohistochemistry

Breast tissue was obtained from routine biopsies evaluated by the pathology department, sectioned at 10 μm on a cryostat, fixed for 5 sec in acetone at room temperature, air dried, and stored at −80 C. Sections were postfixed for 12 min in 4% paraformaldehyde in PBS (pH 7.4) and washed three times in PBS. Nonspecific binding was blocked for 30 min with 10% normal goat serum/0.05% Triton in Tris-buffered saline. The sections were incubated for 1.5 h at room temperature with an affinity-purified OATP-B rabbit antiserum (28), diluted to an IgG concentration of 70 μg/ml in ChemMate diluent (DAKO, Glostrup, Denmark) with 0.05% Triton. Control experiments were performed by incubating sections with normal rabbit IgG and by preadsorption of the antiserum with 20 μg/ml of the antigenic peptide. Sections were washed three times with PBS, incubated for 30 min at room temperature with a Cy2-conjugated $F(ab')_2$ fragment goat antirabbit IgG (Jackson Immuno-Research, West Grove, PA), diluted to 3 μg/ml in DAKO ChemMate diluent, then washed (three times) in PBS. Finally, sections were incubated for 2 min in 5 mM 4′-6-diamidino-2-phenylindole (DAPI), washed with PBS, briefly rinsed with water, then mounted with fluorescent

TABLE 1. Detection of RT-PCR transcripts of the OATP and organic anion transporter gene superfamilies in normal human mammary RNA

Gene	Transporter	Primer sequence forward (5′ → 3′)	Primer sequence reverse (5′ → 3′)	Transcript
OATPs				
SLC21A3	OATP-A	CTTCAGTTGTTGGAATAAATACC	TTCACCAGGTAGATGACACTTCC	+
SLC21A9	OATP-B	CATGGGACCCAGGATAGGGCCAGCG	GGCCTGGCCCCATCATGGTCACTG	+
SLC21A6	OATP-C	CAATCATGGACCAAAATCAACATTTG	GGTTATGACTCCCAATAAGATGTTAG	−
SLC21A11	OATP-D	GCTGAGAACGCAACCGTGGTTCC	GACTTGAGTTCAGGGCTGACTGTCC	+
SLC21A12	OATP-E	GCCATGCCACTGCAGGGAAATG	TTCTGGTACACCAAGCAGGAGCCC	+
SLC21A14	OATP-F	CAGAAAGACAATGGATGTCC	CACATCTTTTAAATCCCCATTTGAGGC	+
SLC21A8	OATP8	GAATAAAACAGCAGAGTCAGCATC	GCAATATAGCTGAATGACAGG	−
SLC21A2	PGT	CCGCAGGGACTGCTCGT	CGCATCAACAAGAACTGCACC	−
OATs				
SLC22A6	OAT1	CATCTACCATCGTGACTGAGTGG	CCTCCATACTCAATTTGGCTCCTTC	−
SLC22A7	OAT2	GAGTACGACCACTCAGAATTCTCC	GGAACAGGTCTAGGTATGAAGGTC	−
SLC22A8	OAT3	GTTCCTGCATGTAGCCATACTGG	GCAGAATGAACTGGCCAAAGGTG	−
SLC22A11	OAT4	CTCTGCGGTTTCCACAAACATGACC	CCACCATCAGTGTCAGTGAACTCAG	−

RT-PCR was performed using total RNA from normal mammary gland as a template. Primers and PCR conditions specific for each transporter are described in *Materials and Methods*. (+), Transcript present; (−), no transcript detectable.

mounting medium (DAKO) and examined by confocal laser scanning microscopy (Leica, Wetzlar, Germany). For double-labeled immunofluorescence, one of the following primary antibodies was included: mouse monoclonal antihuman cytokeratin AE1/AE3 (DAKO), 1.74 μg/ml; mouse monoclonal antihuman calponin Ab-1, clone CALP (NeoMarkers, Fremont, CA), 2 μg/ml; or mouse monoclonal antihuman Ki-67 antigen, clone MIB-1 (DAKO), 700 μg/ml. The Alexa Fluor 647-conjugated $F(ab')_2$ fragment of goat antimouse IgG (Molecular Probes, Eugene, OR), 2.5 μg/ml, served as the secondary antibody.

Stable transfection of OATP-B in CHO-K1 cells

Chinese hamster ovary (CHO)-K1 cells were cultured in DMEM (Life Technologies) supplemented with 10% fetal calf serum, 2 mmol/liter L-glutamine, 50 μg/ml L-proline, 100 U/ml penicillin, and 100 μg/ml streptomycin at 37 C with 5% CO_2 and 95% humidity. Selective medium contained 500 μg/ml G418 sulfate (Life Technologies). The OATP-B open reading frame, originally cloned from human brain (19), was directionally subcloned into the pIRESneo2 (Clontech) expression vector and transfected into CHO-K1 wild-type cells by electroporation as follows: subconfluent CHO-K1 cells were trypsinized and resuspended in cell culture medium. Approximatively 10^7 cells were transferred to a 0.4-cm Gene Pulser cuvette (Bio-Rad, Hercules, CA), mixed with 20 μg plasmid and incubated for 10 min on ice before electroporation using a single electrical pulse with an initial field strength of 250 V, discharged from the 960-μF capacitor (Bio-Rad). After a 10-min incubation on ice, the cells were plated on 10-cm culture dishes, then selected in G418 (1000 μg/ml). Single clones were isolated from the transfected cell pool using cloning cylinders and tested for sodium-independent E_1S uptake. The clone with the highest transport activity was selected.

For immunofluorescent detection of OATP-B in stably transfected CHO-K1 cells grown on glass coverslips, sodium butyrate (5 mmol/liter) was added to the culture medium for 24 h. Cells were fixed in 4% paraformaldehyde for 1 h, permeabilized for 10 min with saponin (0.1%) in PBS, and blocked with gelatin (2%) and BSA (1%) in PBS containing 0.1% saponin for 40 min, then incubated with OATP-B antiserum, diluted to 6 μg IgG per milliliter in PBS with 0.1% saponin and 1% BSA. The Cy2-conjugated $F(ab')_2$ fragment goat antirabbit secondary antibody was diluted in PBS with 1% BSA.

Transport assays

The uptake of radiolabeled substrates in OATP-B transfected CHO cells was measured in triplicate, as follows: cells were grown to confluency on 35-mm dishes and stimulated for 24 h with 5 mmol/liter sodium butyrate (29). Individual dishes were rinsed three times with prewarmed (37 C) uptake buffer consisting of 116 mmol/liter NaCl, 5.3 mmol/liter KCl, 1 mmol/liter NaH_2PO_4, 0.8 mmol/liter $MgSO_4$, 5.5 mmol/liter D-glucose, and 20 mmol/liter HEPES (pH 7.4). Uptake experiments were performed in 800 μl solution containing 0.2–0.3 μCi tritiated substrate supplemented with unlabeled compound to reach the indicated concentrations. Transport was stopped with 2 ml of ice-cold buffer (116 mmol/liter choline Cl, 5.3 mmol/liter KCl, 1 mmol/liter KH_2PO_4, 0.8 mmol/liter $MgSO_4$, 5.5 mmol/liter D-glucose, and 20 mmol/liter HEPES), followed by three additional washes. The cells were solubilized in 1 ml of 1% Triton, and the radioactivity was measured by liquid scintillation counting. Specific OATP-B-mediated uptake was determined by subtracting values from identical experiments conducted in wild-type CHO cells.

Real time quantitative PCR

Total RNA was extracted from the breast cancer cell line T-47D (American Type Culture Collection, Manassas, VA), CHO-K1 wild-type cells, and OATP-B stable transfected CHO cells using the TRIzol Reagent (Life Technologies). Additional RNA from the breast cell lines MCF-7 and MDA-MB-453 and the hepatocyte cell line Hep-G2 was purchased from Ambion, Inc. (Austin, TX). Reverse transcription of 2 μg total RNA was performed with random hexamer primers and 125 U reverse transcriptase (MultiScribe, Applied Biosystems, Rotkreuz, Switzerland). An aliquot (50 ng) was used as a template for real-time PCR (TaqMan, ABI PRISM 7700 Sequence Detector, Applied Biosystems). Primers and the VIC dye-labeled probe for 18S ribosomal RNA, which served as the internal control, were provided by Applied Biosystem. The primers and probe that detected OATP-B have been characterized previously (28): forward primer 5′-AGGACGTGCGGCCAAGT-3′, reverse primer 5′-TCTTTAGGTAGCCGGAGATCATG-3′, FAM/TAMRA-labeled probe 5′-CATCAAGCTGTTCGTTCTGTGCCACA-3′. To detect OATP-D, the following were designed: forward primer 5′-GGTGTCCACTGCTTGCTACGT-3′, reverse primer 5′-TCGGTTTGGCATTCACAGTTATT-3′, FAM/TAMRA-labeled probe 5′-AACAGCACAGCACCTGGCTCAGCC-3′. To detect OATP-E, the following were designed: forward primer 5′-GCGAGCAACCCGGACTT-3′, reverse primer ACATGCCGGTGATGAGAGTG-3′, FAM/TAMRA-labeled probe 5′-AGACCTGCCTCTCTCCATCTGGCTCC-3′.

Results

Detection of OATs in human mammary gland by RT-PCR and Northern blot analysis

RT-PCR of total RNA from normal mammary gland detected transcripts for the following carriers: OATP-A, OATP-B, OATP-D, OATP-E, and OATP-F. The liver-specific carriers, OATP-C and OATP-8, and the related PG transporter (*SLC21A2*) were not present, nor was expression of transporters belonging to the OAT family detected (Table 1). Subsequent Northern blot analyses (Fig. 1) confirmed the presence of OATP-B, which showed a major hybridization signal at 4 kb and a minor band at 1.7 kb after 2 d of exposure. OATP-D and OATP-E showed weaker signals at 3.8 kb and 3.3 kb, respectively, but required exposure for 5 d. Signals for OATP-A and OATP-F could not be detected by Northern blotting, suggesting a very low abundance.

Immunofluorescent localization of OATP-B in the mammary gland

Because of the apparent abundance at the RNA level relative to the other carriers tested, OATP-B was chosen for further characterization. OATP-B was immunolocalized in frozen sections from biopsy material. In tissue with normal appearance, cut from the edges of tumor regions, the OATP-B immunolabeling was weak and discontinuous, and

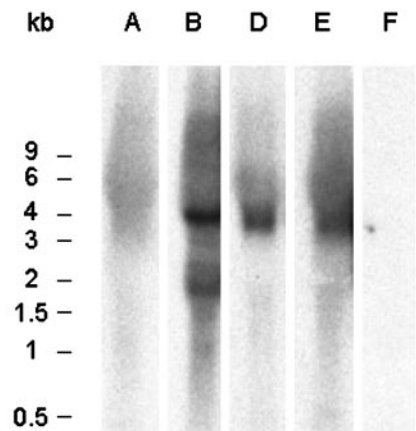

FIG. 1. Northern blot analysis of OATP expression in human breast tissue. Twenty micrograms of total RNA from normal mammary gland were transferred to a nylon membrane and hybridized overnight with a specific antisense-RNA probe for OATP-A (A), OATP-B (B), OATP-D (D), OATP-E (E), and OATP-F (F), as described in *Materials and Methods*. Blots were washed with high stringency and exposed to autoradiographic film at −70 C for 2 d (OATP-B) or 5 d (OATP-A, OATP-D, OATP-E, OATP-F).

confined to the membranes of the external cell layer that surround the ductules (Fig. 2A). Control sections incubated with the preadsorbed OATP-B antibody were negative (Fig. 2B). Normal ductal epithelial cells did not show a signal.

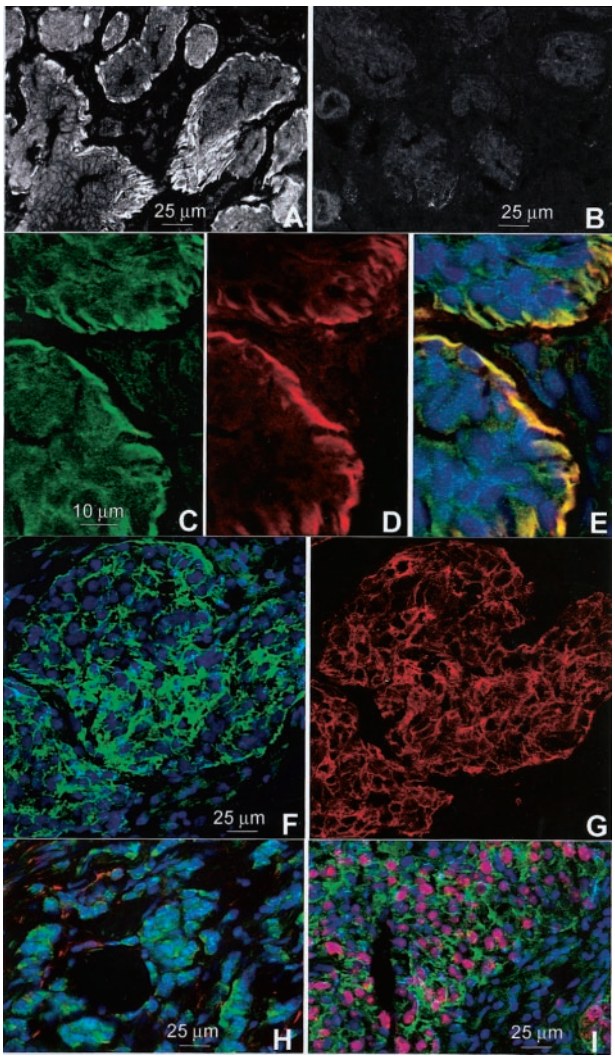

FIG. 2. Immunolocalization of OATP-B in human mammary gland. Cryosections (10 μm) of grossly normal tissue from areas adjacent to an invasive carcinoma (A–E) and sections of invasive carcinoma (F–I) were incubated with primary antibodies and Cy2- or Cy5-conjugated secondary antibodies and examined by confocal scanning microscopy. A, Staining for OATP-B is restricted to the outer cell layer that surrounds the ducts. B, Control slide incubated with OATP-B preadsorbed with the antigenic peptide. C–E, Colocalization of OATP-B (Cy2, *green*) and calponin (Cy5, *red*). C, There is a discontinuous signal for OATP-B (*green*) in the membranes of cells surrounding the ductules. D, An intense signal for calponin (*red*) identifies the myoepithelial cells. E, OATP-B and calponin produce an overlapping signal (*yellow*). Nuclei are counterstained with DAPI (*blue*). F and G, Poorly differentiated invasive ductal carcinoma expresses OATP-B (Cy2, *green*) (F) in the membranes of cytokeratin-positive epithelial cells (Cy5, *red*) (G). Nuclei are counterstained with DAPI (*blue*). H, OATP-B (Cy2, *green*) is expressed in an invasive lobular tumor. The occasional stromal myofibroblast stains for calponin (Cy5, *red*). I, Invasive ductal carcinoma with actively proliferating neoplastic cells staining positive for Ki67 nuclear antigen (Cy5, *red*). OATP-B (Cy2, *green*) is expressed in the proliferating cells. Nuclei are counterstained with DAPI (*blue*).

Morphologically, the cells displaying the positive OATP-B signal were characteristic of the contractile myoepithelial cells that line the ducts of the mammary gland. Double labeling with an antibody to calponin, a smooth muscle cell-specific protein that is a differentiation marker for myoepithelial cells of the breast (30), confirmed the colocalization of calponin and OATP-B to the same cell type (Fig. 2, C–E). In tumor-bearing tissue, OATP-B was most apparent in areas of invasive ductal carcinoma, where it was localized to the membrane of cytokeratin-positive epithelial cells (Fig. 2, F and G) but lost its association with myoepithelial cells (Fig. 2H). OATP-B also retained its membrane expression in neoplastic cells that displayed a positive reaction to the Ki-67 antigen, an indicator of cells in an active proliferating state (Fig. 2I).

Immunolocalization and transport activity of recombinant OATP-B in transfectants

To confirm the membrane expression of OATP-B in stably transfected CHO cells, we immunolocalized the protein after induction of transcription with sodium butyrate. The uniform, positive surface staining indicated marked expression at the plasma membrane (Fig. 3). Wild-type cells were negative (data not shown).

OATP-B mediates E_1S uptake when expressed in oocytes (19) and in HEK293 cells (31) with affinity constant (K_m) values estimated to be 4–6 μmol/liter. However, the assignment of DHEAS as a substrate is equivocal, and the extent of its interaction with other steroids has not been investigated. The validity of the OATP-B stably transfected CHO expression system was first tested for E_1S. Uptake was linear for 20 sec (Fig. 4A) and saturable with an apparent K_m value of 5 μmol/liter and a maximum velocity (V_{max}) value of 777 pmol/mg protein·min (Fig. 4B). In *cis*-inhibition studies with 5 μmol/liter [^{3}H]-E_1S, DHEAS showed a dose-dependent effect that reached statistical significance at 50 μmol/liter (Fig. 5A). Another adrenally derived steroid hormone precursor, pregnenolone sulfate, was a more potent inhibitor and significantly inhibited E_1S uptake to 50% and 20% of control values at 10 μmol/liter and 50 μmol/liter, respectively. Other pregnenolone derivatives, 17-OH pregnenolone sulfate and 21-OH pregnenolone sulfate, inhibited uptake to a moderate degree at the higher concentration tested (Fig. 5B). The unconjugated forms of pregnenolone, 17-OH pregnenolone and 21-OH pregnenolone, exerted no effect when tested at 10 μmol/liter (data not shown).

The inhibition by DHEAS and earlier findings that OATP-B-injected oocytes displayed a 1.6-fold signal over control oocytes (19) imply that DHEAS is a weak substrate for this carrier. Because of the importance of DHEAS as an estrogen precursor, the uptake of [^{3}H]-DHEAS was reevaluated in the OATP-B expressing CHO cells. A significant uptake rate was measurable and showed linearity for 40 sec (Fig. 6A). Nevertheless, the OATP-B-specific signal was weak and displayed large variations when the difference ($uptake_{OATP\text{-}B} - uptake_{wild\text{-}type}$) was calculated (Fig. 6B). To confirm that DHEAS uptake in OATP-B-transfected CHO cells was carrier-mediated over a broad concentration range, equation 1, describing saturable Michaelis-Menten kinetics with a non-

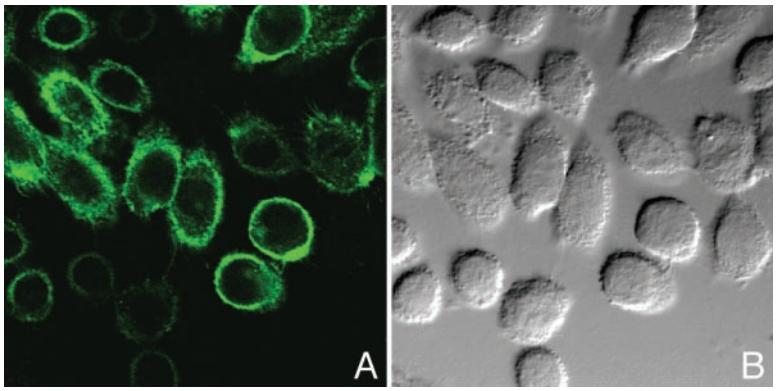

FIG. 3. Immunofluoresence of recombinant OATP-B in stably transfected CHO cells. Wild-type control CHO cells or OATP-B expressing CHO cells were grown on coverslips and incubated for 24 h with 5 mmol/liter sodium butyrate. Sections were stained with an affinity-purified OATP-B-specific antibody and a Cy2-conjugated secondary antibody. A, OATP-B was expressed at the plasma membrane. B, Differential interference contrast of cells shown in A.

saturable first-order process, and equation 2, which describes simple nonsaturable first-order kinetics, were curve-fitted to the data.

$$\upsilon = \frac{V_{max} \cdot [S]}{K_m + [S]} + P \cdot [S] \quad (1)$$

$$\upsilon = P \cdot [S] \quad (2)$$

where υ is the initial rate of uptake (pmol/min·mg), [S] is the substrate concentration (μmol/liter), and P represents a first-order clearance term (μl/min·mg). The background signal in wild-type CHO cells was well described by equation 2. Total DHEAS uptake in OATP-B transfectants was best described by a saturable component plus a first-order process (equation 1) (Fig. 6B). The statistical improvement of the curve fit of equation 1 over equation 2 was assessed by the F test ($F < 0.01$). The estimated K_m and V_{max} values calculated in this way were 9 μmol/liter and 85 pmol/min·mg, respectively, consistent with the fact that OATP-B has moderate affinity but low capacity for DHEAS. Conversely, no OATP-B-mediated uptake of [^{3}H]-pregnenolone sulfate could be identified (data not shown), despite the strong inhibition of E_1S transport by this steroid (Fig. 5).

The interaction of OATP-B and PG

Additional physiological substrates of OATP-B could influence the extent of steroid sulfate uptake in mammary tissue. OATP-B shares 76% identity with the PG transporter (*SLC21A2*), and other more distantly related members of the solute carrier family *21A*, such as OATP-C, do transport PG (21). PGE_2 is especially relevant as a potential substrate for OATP-B because high intratumoral levels are achieved via the cyclooxygenase pathway that is up-regulated in tumors relative to the surrounding normal tissue (32). The role of OATP-B in PG transport was reevaluated in the stable-transfected CHO cells. Neither PGE_1 nor PGE_2 inhibited [^{3}H]-E_1S uptake (Fig. 7A). Additional experiments with radiolabeled PGE_1 and PGE_2 confirmed that OATP-B did not mediate the uptake of PG (data not shown). Unexpectedly, the naturally occurring cyclopentenone PGA_1, which is derived from PGE_1, increased OATP-B-mediated [^{3}H]-E_1S transport (Fig. 7A). The PGA_1-mediated stimulation was detectable after 15 sec and was maximal at 1 min (Fig. 7B). No further stimulation occurred when transport was measured at longer intervals or when cells were preincubated with PGA_1 (data

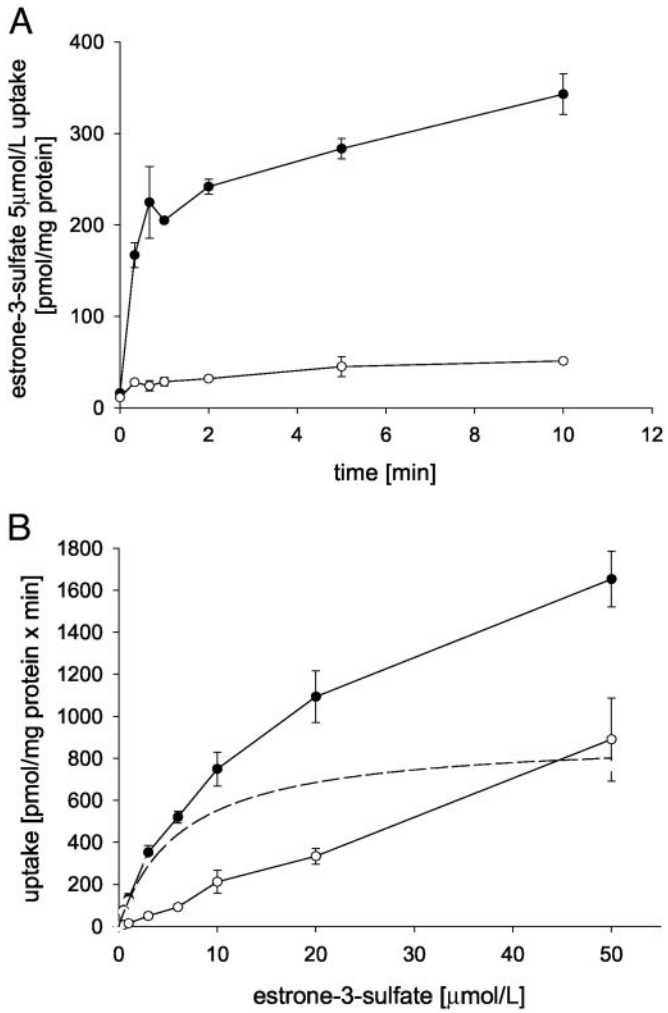

FIG. 4. Time course (A) and saturation kinetics (B) of OATP-B-mediated E_1S uptake into stably transfected CHO-K1 cells. A, After a 24-h incubation in 5 mmol/liter sodium butyrate, wild-type CHO cells (○) or OATP-B-expressing CHO cells (●) were incubated with 5 μmol/liter [^{3}H]-E_1S at 37 C for the indicated times. Data points represent means ± SD of triplicate determinations. B, Wild-type (○) or OATP-B transfected (●) CHO cells were incubated with increasing concentrations of [^{3}H]-E_1S at 37 C for 15 sec. Net OATP-B-mediated uptake (*dashed line*) was calculated by subtracting the values of the wild-type cells from those obtained with the OATP-B transfected cells (means ± SD of three determinations). The data were fitted to the Michaelis-Menten equation using nonlinear regression analysis.

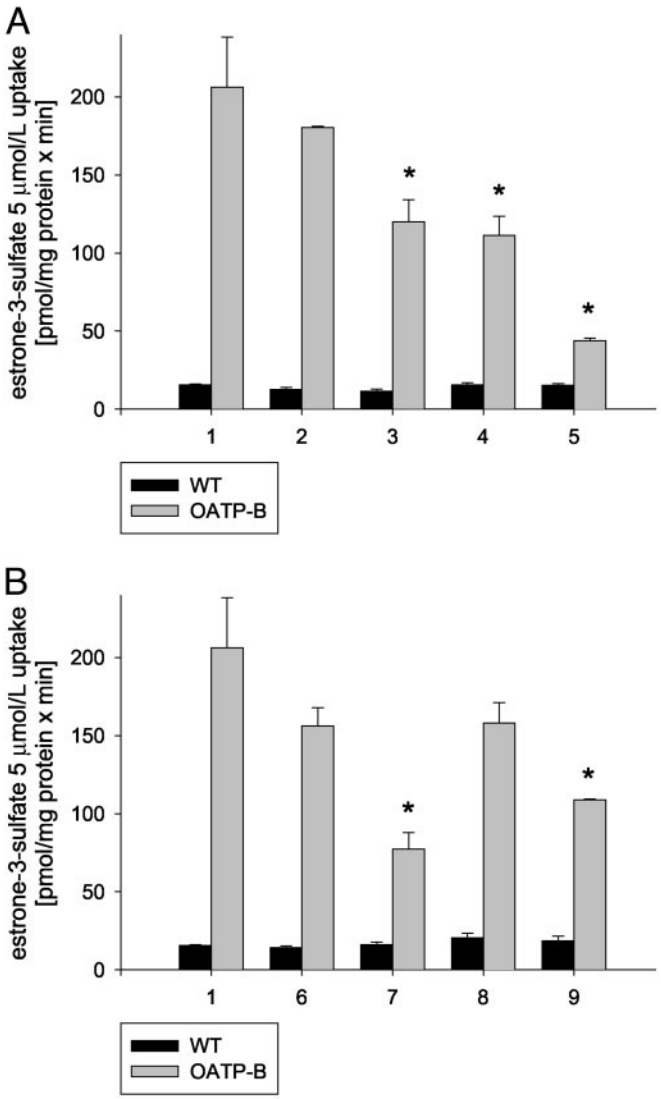

FIG. 5. *cis*-Inhibition of OATP-B-mediated E_1S uptake by steroid sulfates in stably transfected CHO cells. Wild-type (WT; ■) and OATP-B-transfected (▨) CHO cells were grown to confluency on 35-mm dishes and incubated for 24 h in 5 mmol/liter sodium butyrate. Five micromoles per liter of [^{3}H]-E_1S uptake at 37 C were measured in the absence (control) or presence of inhibitors. Data represent the means ± SD of triplicate determinations. *, $P < 0.02$. A: 1, Control; 2, DHEAS, 10 μmol/liter; 3, DHEAS, 50 μmol/liter; 4, pregnenolone sulfate, 10 μmol/liter; 5, pregnenolone sulfate, 50 μmol/liter. B: 1, Control; 6, 21-hydroxy-pregnenolone sulfate, 10 μmol/liter; 7, 21-hydroxy-pregnenolone sulfate, 50 μmol/liter; 8, 17-hydroxy-pregnenolone sulfate, 10 μmol/liter; 9, 17-hydroxy-pregnenolone sulfate, 50 μmol/liter.

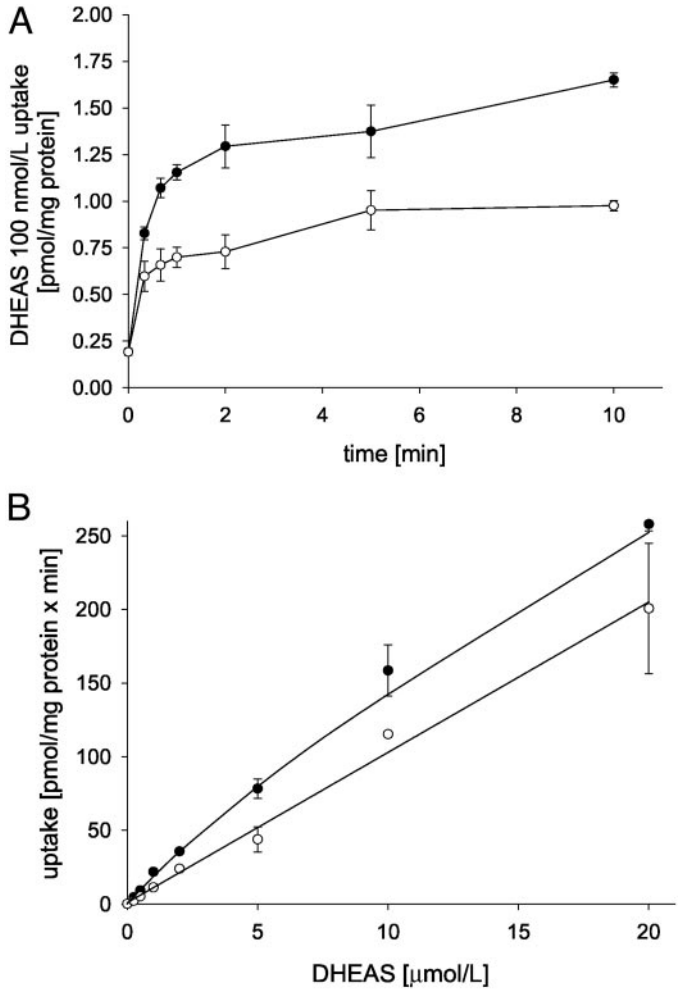

FIG. 6. Time course (A) and saturation kinetics (B) of OATP-B-mediated DHEAS uptake into stably transfected CHO cells. A, After a 24-h incubation in 5 mmol/liter sodium butyrate, wild-type CHO cells (○) or OATP-B expressing CHO cells (●) were incubated with 100 nmol/liter [^{3}H]-DHEAS at 37 C for the indicated times. Data points are means ± SD of triplicate determinations. B, Wild-type (○) or OATP-B-transfected (●) CHO cells were incubated with increasing concentrations of [^{3}H]-DHEAS at 37 C for 30 sec. Data were fitted by nonlinear regression to a model comprising a saturable and first-order component (see equation 2).

not shown). A more marked stimulation was observed at lower substrate concentrations (500 nmol/liter) with both 100 nmol/liter and 1 μmol/liter (Fig. 7B). PGA_2, a second cyclopentenone prostanoid derived from PGE_2, also enhanced E_1S uptake at similar concentrations. However, PGJ_2, a third cyclopentenone PG, which differs from the PG of the A series by the position of the reactive electrophilic carbon, had no effect (Fig. 7C). The PGA_1 and PGA_2 stimulation of transport was also manifest with DHEAS and to the same extent (an increase of 100% ± 5 and 100% ± 10 for PGA_1 and PGA_2, respectively) (Fig. 7D).

To further characterize the PGA-stimulated steroid sulfate transport, the estimation of kinetic parameters was repeated in the presence of 1 μmol/liter PGA_1. There was no difference in the K_m value for either substrate, but the V_{max} increased by 2-fold for DHEAS (from 85 ± 20 to 166 ± 19 pmol/min·mg) and 1.5-fold for E_1S (from 777 ± 45 to 1191 ± 36 pmol/min·mg). To determine whether PGA was a substrate for OATP-B and able to effect stimulation of transport from the *trans*-side of the cell, we measured the time-dependent uptake of [^{3}H]-PGA_1. No OATP-B-mediated uptake of PGA_1 occurred (Fig. 8A). However, a significant signal was evident with both the OATP-B transfectants and wild-type cells, which could represent an element of membrane binding of the radiolabel.

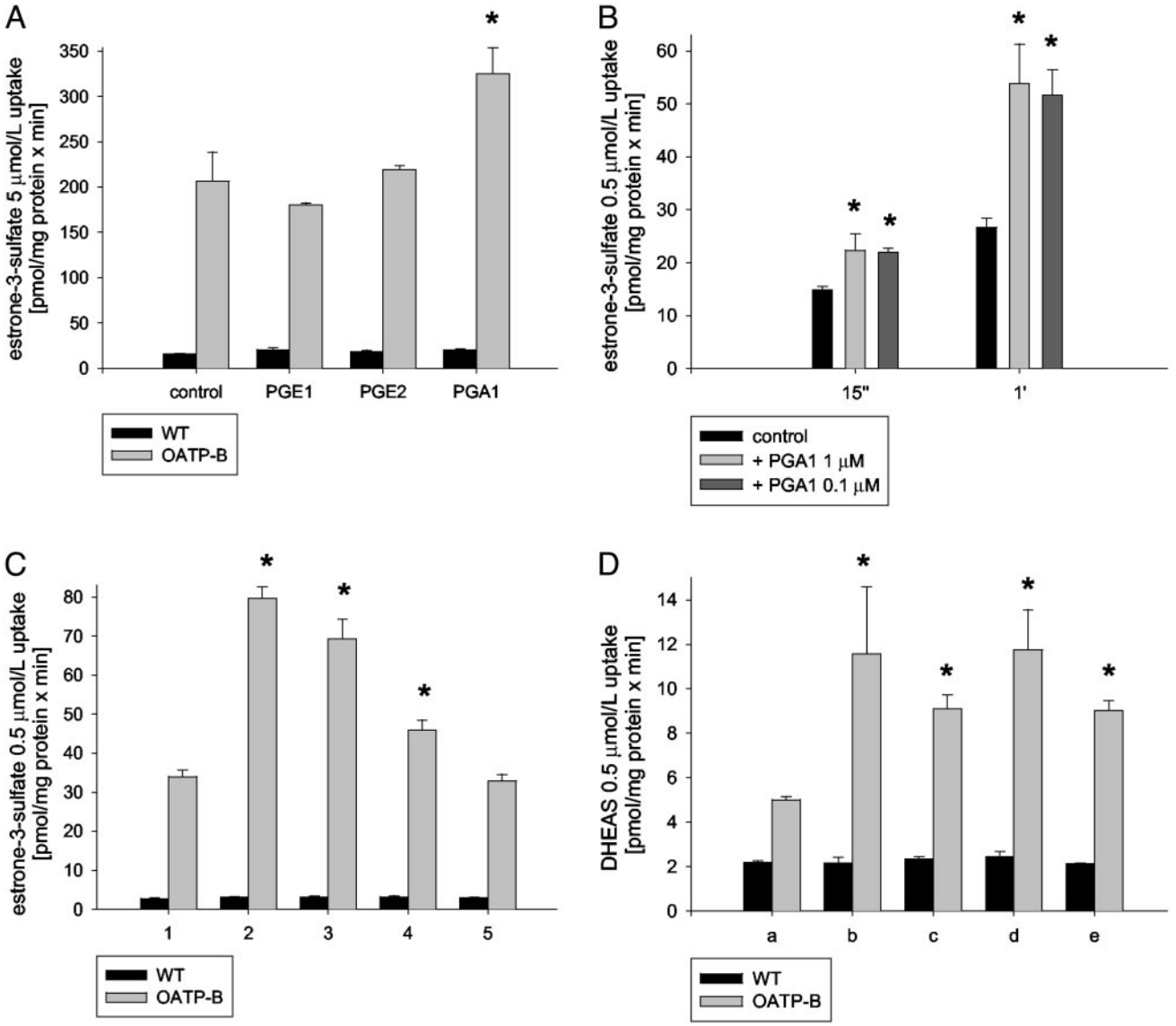

FIG. 7. Effect of PG on OATP-B-mediated E_1S (A–C) and DHEAS (D) uptake. Wild-type (WT) or OATP-B-transfected CHO cells were grown to confluency on 35-mm dishes and incubated for 24 h in 5 mmol/liter sodium butyrate. Uptake of 5 μmol/liter (A), 0.5 μmol/liter (B and C) [^{3}H]-E_1S or 0.5 μmol/liter [^{3}H]-DHEAS (D) was measured at 37 C for 1 min. Data are the means ± SD of triplicate determinations. *, $P < 0.02$. A, 5 μmol/liter [^{3}H]-E_1S in the absence (control) or presence of PGE_1, 10 μmol/liter; PGE_2, 10 μmol/liter; or PGA_1, 10 μmol/liter. B, Fifteen-second or 1-min uptake of 0.5 μmol/liter [^{3}H]-E_1S in the absence (control) or presence of PGA_1, 1 μmol/liter or 0.1 μmol/liter, respectively. C, One-minute uptake of 0.5 μmol/liter [^{3}H]-E_1S in the absence (control, 1) or presence of 1 μmol/liter PGA_1 (2), 1 μmol/liter PGA_2 (3), 0.1 μmol/liter PGA_2 (4), or 1 μmol/liter PGJ_2 (5). D, One-minute uptake of [^{3}H]-DHEAS in the absence (control, a) or presence of 1 μmol/liter PGA_1 (b), 0.1 μmol/liter PGA_1 (c), 1 μmol/liter PGA_2 (d), or 0.1 μmol/liter PGA_2 (e).

The stimulation by PGA_1 and PGA_2 and not PGE_1 and PGE_2 suggests that the cyclopentenone moiety of the compound with its α,β-unsaturated carbonyl group (Fig. 9), is a key determinant of this activity. Accordingly, cyclopentenone (2-cyclopenten-1-one) itself should mimic the effect of PGA. To test this, E_1S uptake was measured in the presence of 50 μmol/liter and 100 μmol/liter cyclopentenone, which resulted in a 1.3-fold and 1.5-fold increase, respectively, in the signal (Fig. 8B). This suggests that the mechanistic basis for the PGA stimulation is the chemical reactivity of the cyclopentenone ring. In particular, the electrophilic C_{11} of PGA_1 and PGA_2 (Fig. 9) is susceptible to addition reactions with nucleophiles such as the free sulfhydryl group of cysteine residues (33). To investigate whether Cys residues in the OATP-B protein may be target sites for the actions of PGA_1 and PGA_2, transport studies were performed in the presence of thiol reagents. Cells pretreated with 100 μmol/liter of the membrane-permeable NEM showed a 40% decrease in E_1S uptake, suggesting that one or more Cys residues are involved in substrate binding and/or transport (Fig. 8C). In NEM-pretreated cells, the PGA_1 stimulation was completely abrogated. This supports the notion that an interaction with cysteine residues regulates the actions of PGA_1. Additional experiments with the membrane impermeable, polar sulfhydryl reagent IASD at 500 μmol/liter, which accesses only those Cys residues within a hydrophilic

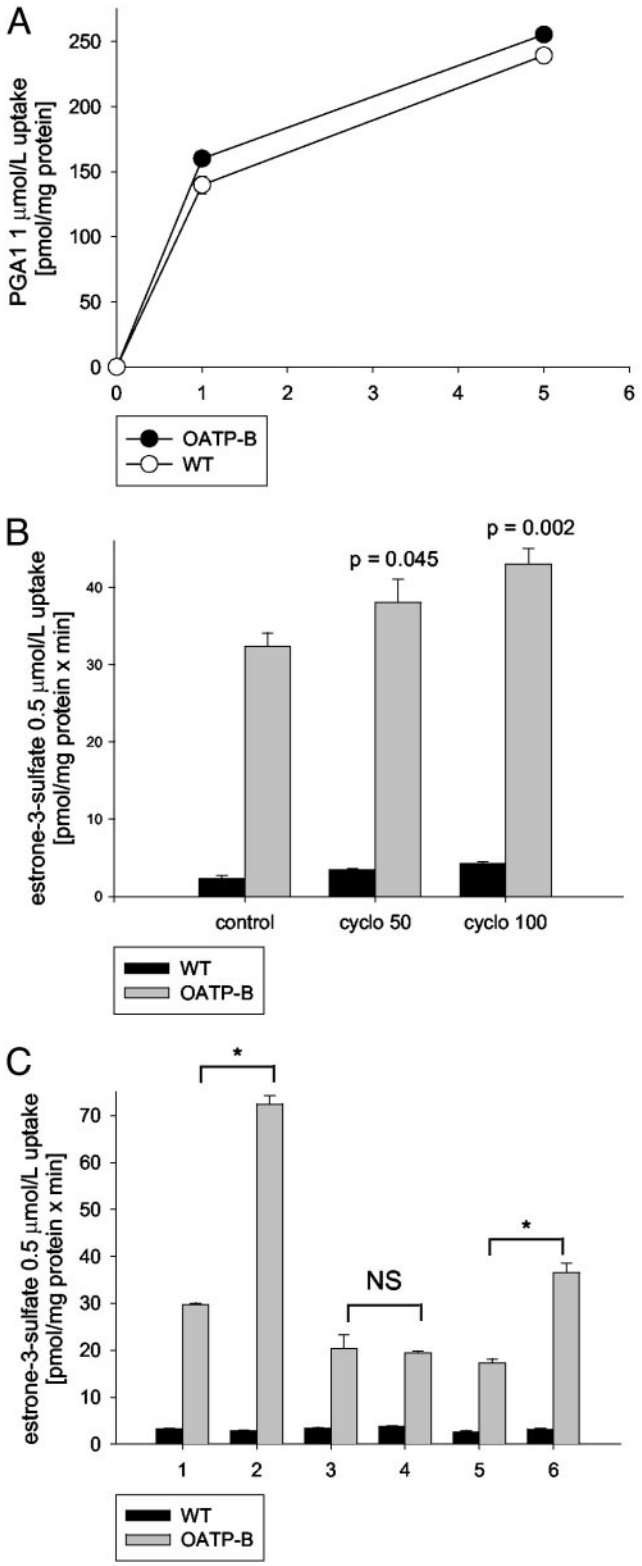

FIG. 8. Interaction of PGA with OATP-B. A, [^{3}H]-PGA_1 was tested as a substrate for OATP-B in wild-type CHO cells (○) and OATP-B transfectants (●) after stimulation for 24 h with sodium butyrate. Uptake was measured at 37 C for 1 min and 5 min. B, The effect of the cyclopentenone moiety of PGA on OATP-B-mediated E_1S uptake. Wild-type CHO (WT) cells (■) and OATP-B transfectants (▨) were incubated with cyclopentenone, and uptake of [^{3}H]-E_1S was measured after 1 min at 37 C. Cyclopentenone at 50 μmol/liter and 100 μmol/liter significantly stimulated transport compared with control conditions (no cyclopentenone). C, The effect of thiol reagents on PGA stimulation of OATP-B transport. E_1S uptake was measured at 1 min in wild-type (■) and OATP-B transfectants (▨) in the absence (bars 1, 3, and 5) and presence of PGA_1 1 μmol/liter (bars 2, 4, and 6). The membrane permeable thiol reagent, NEM (bars 3 and 4) inhibited substrate binding and/or transport. The effect of PGA_1 (bar 4) was blocked. The hydrophilic thiol reagent, IASD acid, also inhibited transport (bars 5 and 6), but transport was stimulated 2-fold by PGA_1 (bar 6). Data are mean ± SD of triplicate determinations.

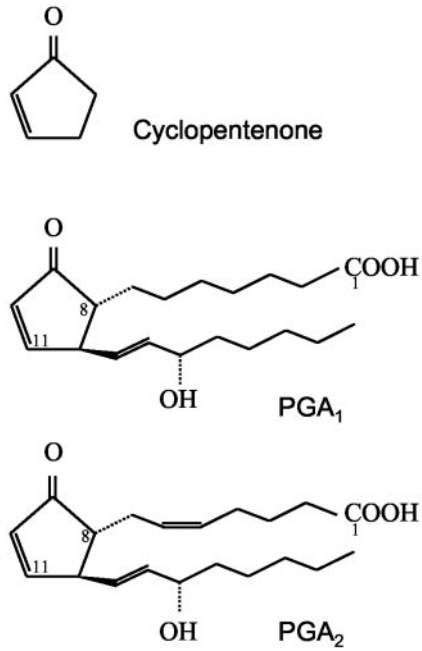

FIG. 9. Cyclopentenone PG. PGA_1 and PGA_2 both contain the cyclopentenone ring structure. The electrophilic carbon (C_{11}) is indicated.

environment, supported this view. E_1S uptake was equally sensitive to the presence of IASD as with NEM (Fig. 8C). However, a 2-fold stimulation with PGA_1 was still possible, in keeping with the hypothesis that the Cys residues reacting with PGA are inaccessible to the hydrophilic IASD but are nevertheless blocked by NEM.

The presence of OATPs in breast cancer cell lines

To establish whether widely used breast cancer cell lines expressed OATP carriers and could serve as *in vitro* models for additional studies of steroid sulfate transport, the mRNA expression of OATP-B, OATP-D, and OATP-E was measured in MCF-7, T47D, and MDA-MB-453 cell lines. For comparison, the expression levels in the OATP-B stably transfected CHO cells as well as in the Hep-G2 cell line, which reportedly expresses both OATP-B and OATP-E (34), are given. None of the breast cancer lines examined gave detectable signals for OATP-B above background levels (Table 2). Conversely, when standardized for expression in Hep-G2 cells, our studies identified MCF-7 as the cell line with the highest expression of OATP-E (13-fold higher than Hep-G2), whereas the MDA-MB-453 and T47-D cell lines express 10-fold and 100-fold less, respectively. Although no standard cell line was

TABLE 2. Real-time quantitative PCR of OATP carriers in human mammary cancer cell lines

Cell line	OATP-B		OATP-E		OATP-D
	ΔC_t[a] OATPB-18S	Relative level[b]	ΔC_t[a] OATPE-18S	Relative level[c]	ΔC_t[a] OATPD-18S
Cell line					
$CHO_{(OATP-B)}$	10.5 ± 0.06	100 ± 2%			
MCF-7	ND		11.5 ± 0.2	1380 ± 44%	15.5 ± 0.2
MDA-MB-453	ND		18.6 ± 0.2	10 ± 3%	24.4 ± 0.6
T47-D	ND		24.8 ± 0.1	0.14 ± 0.004%	21.7 ± 0.1
Hep-G2	16.8 ± 0.5	1.2 ± 0.4%	15.3 ± 0.3	100 ± 30%	

Data are mean ± SD of triplicate measurements. ND, Not detected.

[a] The data were calculated by subtracting the signal threshold cycles (C_t) of the internal standard (ribosomal 18S) from the C_t of the target gene (OATP-B, OATP-E, OATP-D).

[b] Values were normalized to the expression level of OATP-B transfected CHO, set to 100%.

[c] Values were normalized to the expression level of Hep-G2 cells, set to 100%.

available for OATP-D, MCF-7 again expressed the highest levels of OATP-D mRNA (approximately 100-fold more than T47-D and 500-fold more than MDA-MB-453) (Table 2).

Discussion

OATP-B appears to be one of the most abundant organic anion uptake carriers expressed in the human mammary gland. Generally, OATP family members exhibit broad substrate specificity, encompassing bile salts, sulfate, and glucuronide conjugates of endogenous and exogenous compounds, anionic peptides, and even cations in some cases (16). OATP-B is peculiar in that its substrate list is restricted, despite its expression in a broad range of tissues (22). The transport of E_1S remains the best characterized function for this carrier and may represent its true physiological role in the mammary gland.

At the protein level, the expression of OATP-B in normal mammary tissue was confined to the myoepithelium. Myoepithelial cells have contractile properties required for lactation and can elaborate extracellular matrix proteins, such as collagen and laminin, that are needed to maintain polarity in the adjacent ductal epithelial cells (35). The current findings identify OATP-B as a steroid sulfate carrier in the myoepithelium. In view of the recent report that marked steroid sulfatase activity is also present in isolated myoepithelial cells (36), it is tempting to speculate that these cells engage in intercellular cross-talk to supply desulfated hormones to adjacent target cells. OATP-B is also expressed in the epithelia of invasive ductal carcinomas, which are characterized in part by the absence of myoepithelial cells. In these sections, expression was marked in the majority of tumor cells, including those in an active proliferating state. The presence of a steroid sulfate carrier in tumor cells could be a previously unrecognized factor, together with the elevated expression levels of the 17β-hydroxysteroid dehydrogenase type 1 and aromatase enzymes (12, 37), that contributes to the high intratumor levels of E_2 reported in some cases. The influence of OATP-B in determining the estrogen level of target cells will, nevertheless, be tempered by the multidrug resistance protein MRP1, the expression of which in epithelial cells of normal and tumoral breast tissue has been documented (34, 38, 39). MRP1 can export E_1S (40), and, considering the high variability in expression levels detected in cancer patients (38, 39), it could have an unpredictable influence on the status and relevance of OATP-B in breast tumors.

Independent of the eventual conversion to E_2, DHEA itself may exert biological actions on mammary tissue, both on transcription events and through signal transduction mechanisms. There is evidence that DHEA contributes to estrogen receptor-dependent *trans*-activation of transcription (41, 42), and DHEA can inhibit vascular smooth muscle cell proliferation through an inhibition of phosphorylation signaling (43).

Pregnenolone sulfate, an adrenal steroid that serves as a precursor for DHEA and progesterone, achieves circulating concentrations of approximately 1 μmol/liter (44). There is some evidence that the enzymatic pathway from pregnenolone to 17-hydroxypregnenolone to DHEA and androstenedione is intact in human breast tissue (45) and that pregnenolone sulfate can accumulate in fibrocystic breast cyst fluid in concentrations up to 20 times greater than in serum (46). In light of previous findings that pregnenolone sulfate could inhibit OATP-B-mediated E_1S uptake in an oocyte expression system and in basal membrane vesicles isolated from placental syncytiotrophoblast (28), we speculated that OATP-B may be a broad-spectrum steroid sulfate carrier and could accept such a relevant steroid hormone precursor. Despite the clearly evident interaction of pregnenolone sulfate with the OATP-B carrier to inhibit E_1S transport, it is not a substrate. Therefore, OATP-B remains a selective carrier but one that is susceptible to inhibition by other physiological steroids.

The finding that PGA_1 and PGA_2 can stimulate OATP-B-mediated uptake implies that E_1S and DHEAS cellular entry can be regulated locally at the plasma membrane, possibly with downstream consequences of increased hormone exposure in target cells. PGE_2 is a product of arachidonic acid metabolism and is secreted by breast tumor cells as well as stromal cells (47–49). Its formation is catalyzed by cyclooxygenase 2, an enzyme up-regulated in breast cancer tissue. PGA_1 and PGA_2 arise from the dehydration of PGE_1 and PGE_2, respectively, both intracellularly and in the circulation. It follows that PGA_1 and/or PGA_2 are physiologically relevant and available for interaction with the OATP-B carrier. The mode of this interaction requires detailed study, but the present findings emphasize that the reactive cyclopentenone ring and cysteine residues are critical elements (Fig. 8, B and C). PGA can form adducts with selected proteins: PGA_1 covalently binds to IκB kinase to inhibit the phosphorylation of IκBα (50), and PGA_2 binds covalently to Cys 47 of the

glutathione S-transferase P1 isozyme (51). Therefore, a reaction between PGA_1/PGA_2 and one or more cysteine residue of OATP-B can be counted as a plausible mechanism but one that must accommodate a resulting increase in activity rather than a decrease. As with the other members of the human OATP superfamily, OATP-B has several Cys residues within the purported extracellular domains (16). It is likely that one or more are important for substrate binding and transport because E_1S uptake is sensitive to the thiol reagents, NEM and IASD. PGA_1 remains effective in the presence of the impermeable IASD, suggesting that PGA_1 is acting at a distinct site, inaccessible to the hydrophilic reagent but vulnerable to the more lipophilic PG. The mechanism by which the proposed PGA_1-OATP-B interaction stimulates transport has not been addressed here. One reasonable hypothesis involves consideration of the quaternary structure of this integral membrane protein. OATP-B has 12 putative membrane-spanning domains, a characteristic it shares with all members of the solute carrier family *SLC21A* (16). Other membrane transporters with a similar 12 *trans*-membrane domain structure, such as glucose transporter type 1 belonging to the *SLC2A* solute carrier family and the serotonin and dopamine transporters that are members of the *SLC6A* family, form oligomers mediated by disulfide bonds. A change in the state of oligomerization carries functional consequences (52, 53). If OATP-B shares these biochemical features, it is possible that PGA could intervene at critical Cys residues to induce a more favorable oligomeric structure.

OATP-B was not expressed in three widely used, phenotypically characterized breast cancer cell lines (Table 2). This precludes their fortuitous use as model cell lines in which to conduct additional regulatory studies against backgrounds of varying steroid hormone receptor levels and metabolic pathways. The lack of OATP-B notwithstanding, both MCF-7 and T47-D cells respond positively to exposure to E_1S and DHEAS, with changes in downstream metabolites and growth (4, 54, 55). The fact that both cell lines express OATP-D and OATP-E to some degree (Table 2) and that E_1S is listed as a weak substrate for both of these carriers (22) could account for this. Whether OATP- D and OATP-E have a role in determining steroid hormone levels in human breast tissue has yet to be examined.

The perceived risk of estrogen exposure in the genesis and progression of breast cancer is strong. In light of the current findings, additional studies that specifically address 1) the comparative expression of OATP-B in breast tumors and normal tissue and 2) the possible coordinate regulation of this carrier with enzymes that metabolize precursors to downstream, biologically active hormones, are warranted. Moreover, the possibility that the interaction with PG of the A series constitutes a point of regulation for the actions of OATP-B in breast tissue merits further consideration.

Acknowledgments

We are grateful for the help provided by Dr. Matthias Hoechli and the use of the facilities of the Electron Microscopy Laboratory, University of Zürich.

Received February 3, 2003. Accepted April 24, 2003.

Address all correspondence and requests for reprints to: M. V. St-Pierre, Ph.D., Division of Clinical Pharmacology and Toxicology, Department of Internal Medicine, University Hospital Zürich, 100 Rämistrasse, Zürich 8091, Switzerland. E-mail: stpierre@kpt.unizh.ch.

This work was supported by Grant 01B38 from the Novartis Foundation for Biomedical Research (to M.V.S.-P.), a grant from the University of Zürich Forschungskommission (to M.V.S.-P.), and grants from the National Science Foundation, Switzerland (31-67173.01, to M.V.S.-P.; and 31-64140.00, to P.J.M.).

References

1. **Russo J, Hu YF, Silva ID, Russo IH** 2001 Cancer risk related to mammary gland structure and development. Microsc Res Tech 2001 52:204–223
2. **Katzenellenbogen BS, Katzenellenbogen JA** 2000 Estrogen receptor transcription and transactivation: estrogen receptor α and estrogen receptor β: regulation by selective estrogen receptor modulators and importance in breast cancer. Breast Cancer Res 2:335–344
3. **Labrie F, Belanger A, Luu-The V, Labrie C, Simard J, Cusan L, Gomez JL, Candas B** 1998 DHEA and the intracrine formation of androgens and estrogens in peripheral target tissues: its role during aging. Steroids 63:322–328
4. **Morris KT, Toth-Fejel S, Schmidt J, Fletcher WS, Pommier RF** 2001 High dehydroepiandrosterone-sulfate predicts breast cancer progression during new aromatase inhibitor therapy and stimulates breast cancer cell growth in tissue culture: a renewed role for adrenalectomy. Surgery 130:947–953
5. **Schmitt M, Klinga K, Schnarr B, Morfin R, Mayer D** 2001 Dehydroepiandrosterone stimulates proliferation and gene expression in MCF-7 cells after conversion to estradiol. Mol Cell Endocrinol 173:1–13
6. **Maggiolini M, Bonofiglio D, Pezzi V, Carpino A, Marsico S, Rago V, Vivacqua A, Picard D, Ando S** 2002 Aromatase overexpression enhances the stimulatory effects of adrenal androgens on MCF7 breast cancer cells. Mol Cell Endocrinol 193:13–18
7. **Chetrite GS, Cortes-Prieto J, Philippe JC, Wright F, Pasqualini JR** 2000 Comparison of estrogen concentrations, estrone sulfatase and aromatase activities in normal, and in cancerous, human breast tissues. J Steroid Biochem Mol Biol 72:23–27
8. **Remy-Martin A, Prost O, Nicollier M, Burnod J, Adessi GL** 1983 Estrone sulfate concentrations in plasma of normal individuals, postmenopausal women with breast cancer, and men with cirrhosis. Clin Chem 29:86–89
9. **Platia MP, Fencl MD, Elkind-Hirsch KE, Canick JA, Tulchinsky D** 1984 Estrone sulfatase activity in the human brain and estrone sulfate levels in the normal menstrual cycle. J Steroid Biochem 21:237–241
10. **Soderqvist G, Olsson H, Wilking N, von Schoultz B, Carlstrom K** 1994 Metabolism of estrone sulfate by normal breast tissue: influence of menopausal status and oral contraceptives. J Steroid Biochem Mol Biol 48:221–224
11. **Sulcova J, Hill M, Hampl R, Starka L** 1997 Age and sex related differences in serum levels of unconjugated dehydroepiandrosterone and its sulphate in normal subjects. J Endocrinol 154:57–62
12. **Ariga N, Moriya T, Suzuki T, Kimura M, Ohuchi N, Satomi S, Sasano H** 2000 17β-Hydroxysteroid dehydrogenase type 1 and type 2 in ductal carcinoma in situ and intraductal proliferative lesions of the human breast. Anticancer Res 20:1101–1108
13. **Suzuki T, Moriya T, Ariga N, Kaneko C, Kanazawa M, Sasano H** 2000 17β-Hydroxysteroid dehydrogenase type 1 and type 2 in human breast carcinoma: a correlation to clinicopathological parameters. Br J Cancer 82:518–523
14. **Dorgan JF, Stanczyk FZ, Longcope C, Stephenson Jr HE, Chang L, Miller R, Franz C, Falk RT, Kahle L** 1997 Relationship of serum dehydroepiandrosterone (DHEA), DHEA sulfate, and 5-androstene-3β, 17β-diol to risk of breast cancer in postmenopausal women. Cancer Epidemiol Biomarkers Prev 6: 177–181
15. **Endogenous Hormones and Breast Cancer Collaborative Group** 2002 Endogenous sex hormones and breast cancer in postmenopausal women: reanalysis of nine prospective studies. J Natl Cancer Inst 94:606–616.
16. **Hagenbuch B, Meier PJ** 2003 The superfamily of organic anion transporting polypeptides. Biochim Biophys Acta 1609:1–18
17. **Sweet DH, Bush KT, Nigam SK** 2001 The organic anion transporter family: from physiology to ontogeny and the clinic. Am J Physiol Renal Physiol 281:F197–F205
18. **Kullak-Ublick GA, Fisch T, Oswald M, Hagenbuch B, Meier PJ, Beuers U, Paumgartner G** 1998 Dehydroepiandrosterone sulfate (DHEAS): identification of a carrier protein in human liver and brain. FEBS Lett 424:173–176
19. **Kullak-Ublick GA, Ismair MG, Stieger B, Landmann L, Huber R, Pizzagalli F, Fattinger K, Meier PJ, Hagenbuch B** 2001 Organic anion-transporting polypeptide B (OATP-B) and its functional comparison with three other OATPs of human liver. Gastroenterology 120:525–533
20. **Konig J, Cui Y, Nies AT, Keppler D** 2000 A novel human organic anion transporting polypeptide localized to the basolateral hepatocyte membrane. Am J Physiol Gastrointest Liver Physiol 278:G156–G164
21. **Abe T, Kakyo M, Tokui T, Nakagomi R, Nishio T, Nakai D, Nomura H, Unno M, Suzuki M, Naitoh T, Matsuno S, Yawo H** 1999 Identification of a novel

gene family encoding human liver-specific organic anion transporter LST-1. J Biol Chem 274:17159–17163
22. **Tamai I, Nezu J, Uchino H, Sai Y, Oku A, Shimane M, Tsuji A** 2000 Molecular identification and characterization of novel members of the human organic anion transporter (OATP) family. Biochem Biophys Res Commun 273:251–260
23. **Pizzagalli F, Hagenbuch B, Stieger B, Klenk U, Folkers G, Meier PJ** 2002 Identification of a novel human organic anion transporting polypeptide as a high affinity thyroxine transporter. Mol Endocrinol 16:2283–2296
24. **Cha SH, Sekine T, Fukushima JI, Kanai Y, Kobayashi Y, Goya T, Endou H** 2001 Identification and characterization of human organic anion transporter 3 expressing predominantly in the kidney. Mol Pharmacol 59:1277–1286
25. **Cha SH, Sekine T, Kusuhara H, Yu E, Kim JY, Kim DK, Sugiyama Y, Kanai Y, Endou H** 2000 Molecular cloning and characterization of multispecific organic anion transporter 4 expressed in the placenta. J Biol Chem 275:4507–4512
26. **Motohashi H, Sakurai Y, Saito H, Masuda S, Urakami Y, Goto M, Fukatsu A, Ogawa O, Inui K** 2002 Gene expression levels and immunolocalization of organic ion transporters in the human kidney. J Am Soc Nephrol 13:866–874
27. **Andersen NH** 1969 Dehydration of prostaglandins: study by spectroscopic method. J Lipid Res 10:320–325
28. **St-Pierre MV, Hagenbuch B, Ugele B, Meier PJ, Stallmach T** 2002 Characterization of an organic anion transporting polypeptide OATP B in human placenta. J Clin Endocrinol Metab 87:1856–1863
29. **Palermo DP, DeGraaf ME, Marotti KR, Rehberg E, Post LE** 1991 Production of analytical quantities of recombinant proteins in Chinese hamster ovary cells using sodium butyrate to elevate gene expression. J Biotechnol 19:35–47
30. **Lazard D, Sastre X, Frid MG, Glukhova MA, Thiery JP, Koteliansky VE** 1993 Expression of smooth muscle-specific proteins in myoepithelium and stromal myofibroblasts of normal and malignant human breast tissue. Proc Natl Acad Sci USA 90:999–1003
31. **Tamai I, Nozawa T, Koshida M, Nezu J, Sai Y, Tsuji A** 2001 Functional characterization of human organic anion transporting polypeptide B (OATP-B) in comparison with liver-specific OATP-C. Pharm Res 18:1262–1269
32. **Zhao Y, Agarwal VR, Mendelson CR, Simpson ER** 1996 Estrogen biosynthesis proximal to a breast tumor is stimulated by PGE2 via cyclic AMP, leading to activation of promoter II of the CYP19 (aromatase) gene. Endocrinology 137:5739–5742
33. **Straus DS, Glass CK** 2001 Cyclopentenone prostaglandins: new insights on biological activities and cellular targets. Med Res Rev 21:185–210
34. **Alcorn J, Lu X, Moscow JA, McNamara PJ** 2002 Transporter gene expression in lactating and nonlactating human mammary epithelial cells using real-time reverse transcription-polymerase chain reaction. J Pharmacol Exp Ther 303:487–496
35. **Slade MJ, Coope RC, Gomm JJ, Coombes RC** 1999 The human mammary gland basement membrane is integral to the polarity of luminal epithelial cells. Exp Cell Res 247:267–278
36. **Tobacman JK, Hinkhouse M, Khalkhali-Ellis Z** 2002 Steroid sulfatase activity and expression in mammary myoepithelial cells. J Steroid Biochem Mol Biol 81:65–68
37. **Miyoshi Y, Ando A, Shiba E, Taguchi T, Tamaki Y, Noguchi S** 2001 Involvement of up-regulation of 17 β-hydroxysteroid dehydrogenase type 1 in maintenance of intratumoral high estradiol levels in postmenopausal breast cancers. Int J Cancer 2001 94:685–689
38. **Dexter DW, Reddy RK, Geles KG, Bansal S, Myint MA, Rogakto A, Leighton JC, Goldstein LJ** 1998 Quantitative reverse transcriptase-polymerase chain reaction measured expression of MDR1 and MRP in primary breast carcinoma. Clin Cancer Res 4:1533–1542
39. **Filipits M, Malayeri R, Suchomel RW, Pohl G, Stranzl T, Dekan G, Kaider A, Stiglbauer W, Depisch D, Pirker R** 1999 Expression of the multidrug resistance protein (MRP1) in breast cancer. Anticancer Res 19:5043–5049
40. **Qian YM, Song WC, Cui H, Cole SP, Deeley RG** 2001 Glutathione stimulates sulfated estrogen transport by multidrug resistance protein 1. J Biol Chem 276:6404–6411
41. **Bruder JM, Sobek L, Oettel M** 1997 Dehydroepiandrosterone stimulates the estrogen response element. J Steroid Biochem Mol Biol 62:461–466
42. **Maggiolini M, Donze O, Jeannin E, Ando S, Picard D** 1999 Adrenal androgens stimulate the proliferation of breast cancer cells as direct activators of estrogen receptor α. Cancer Res 59:4864–4869
43. **Williams MR, Ling S, Dawood T, Hashimura K, Dai A, Li H, Liu JP, Funder JW, Sudhir K, Komesaroff PA** 2002 Dehydroepiandrosterone inhibits human vascular smooth muscle cell proliferation independent of ARs and ERs. J Clin Endocrinol Metab 87:176–181
44. **de Peretti E, Mappus E** 1983 Pattern of plasma pregnenolone sulfate levels in humans from birth to adulthood. J Clin Endocrinol Metab 57:550–556
45. **Abul-Hajj YJ, Iverson R, Kiang DT** 1979 Metabolism of pregnenolone by human breast cancer. Evidence for 17α-hydroxylase and 17,20-lyase. Steroids 34:817–827
46. **Maeda Y, Tanaka E, Fujiwara M, Watanabe R, Furusawa H, Matsu T, Nakahara H, Nanba K, Higashi S, Setoguchi T** 2002 Accumulation of 4- and 5-ene steroid sulfates in human breast cyst fluids. J Steroid Biochem Mol Biol 81:249–253
47. **Brueggemeier RW, Quinn AL, Parrett ML, Joarder FS, Harris RE, Robertson FM** 1999 Correlation of aromatase and cyclooxygenase gene expression in human breast cancer specimens. Cancer Lett 140:27–35
48. **Karuppu D, Kalus A, Simpson ER, Clyne C** 2002 Aromatase and prostaglandin inter-relationships in breast adipose tissue: significance for breast cancer development. Breast Cancer Res Treat 76:103–109
49. **Richards JA, Petrel TA, Brueggemeier RW** 2002 Signaling pathways regulating aromatase and cyclooxygenases in normal and malignant breast cells. J Steroid Biochem Mol Biol 80:203–212
50. **Rossi A, Kapahi P, Natoli G, Takahashi T, Chen Y, Karin M, Santoro MG** 2000 Anti-inflammatory cyclopentenone prostaglandins are direct inhibitors of IκB kinase. Nature 403:103–108
51. **van Iersel ML, Cnubben NH, Smink N, Koeman JH, van Bladeren PJ** 1999 Interactions of prostaglandin A2 with the glutathione-mediated biotransformation system. Biochem Pharmacol 57:1383–1390
52. **Sur C, Schloss P, Betz H** 1997 The rat serotonin transporter: identification of cysteine residues important for substrate transport. Biochem Biophys Res Commun 241:68–72
53. **Zottola RJ, Cloherty EK, Coderre PE, Hansen A, Hebert DN, Carruthers A** 1995 Glucose transporter function is controlled by transporter oligomeric structure. A single, intramolecular disulfide promotes GLUT1 tetramerization. Biochemistry 34:9734–9747
54. **MacIndoe JH** 1988 The hydrolysis of estrone sulfate and dehydroepiandrosterone sulfate by MCF-7 human breast cancer cells. Endocrinology 123:1281–1287
55. **Billich A, Nussbaumer P, Lehr P** 2000 Stimulation of MCF-7 breast cancer cell proliferation by estrone sulfate and dehydroepiandrosterone sulfate: inhibition by novel non-steroidal steroid sulfatase inhibitors. J Steroid Biochem Mol Biol 73:225–235